The Astrophysical Journal, 631:L129–L132, 2005 October 1

THE PATTERN SPEEDS OF 38 BARRED GALAXIES

P. Rautiainen, H. Salo, and E. Laurikainen
Department of Physical Sciences, University of Oulu, P.O. Box 3000, FIN-90014 University of Oulu, Finland; pertti.rautiainen@oulu.fi, heikki.salo@oulu.fi, eija.laurikainen@oulu.fi
Received 2005 July 1; accepted 2005 August 25; published 2005 September 21

ABSTRACT

We estimate the pattern speeds of 38 barred galaxies by simulation modeling. We construct the gravitational potentials of the galaxies from near-IR photometry by assuming that the mass-to-light ratio (M/L) is constant in the H band and a single pattern speed dominates in the stellar disk. We use the response of gaseous and stellar particle disks to a rigidly rotating potential to determine the pattern speed. If our assumptions are correct, then the pattern speed depends on the morphological type: the average value of the ratio of the corotation resonance radius to the bar radius, $\mathcal{R}$, increases from about 1.1 in type SB0/a to 1.4 in SBb and 1.7 in SBc. Within the error estimates, all the bars in galaxies of type SBab or earlier are fast rotators, having $\mathcal{R} \leq 1.4$, whereas late-type galaxies include both fast and slow rotators.

Subject headings: galaxies: fundamental parameters — galaxies: kinematics and dynamics — galaxies: structure

1. INTRODUCTION

The pattern speed of a stellar bar ($\Omega_{\rm bar}$) has a physical upper limit, equal to the angular speed of circular rotation at the distance of the bar radius. Thus, the ratio of the corotation resonance (CR) radius to the bar radius (i.e., semilength) $\mathcal{R} = R_{\rm CR}/R_{\rm bar}$ must be equal to or larger than 1.0, because bar-supporting orbits do not exist beyond the corotation resonance (Contopoulos 1980). On the other hand, there is no evident lower limit for the bar pattern speed. The often-used nomenclature is based on the value of $\mathcal{R}$: if $\mathcal{R} \leq 1.4$, the bar is "fast"; otherwise, it is "slow" (Debattista & Sellwood 2000).

N-body simulations in which a bar forms by a global bar instability tend to produce fast bars (Sellwood 1981). Secular evolution, especially the interaction between the bar and the dark halo, can decelerate an initially fast-rotating bar so much that it becomes a slow rotator (Debattista & Sellwood 1998; Athanassoula 2003). On the other hand, if a bar forms more gradually, or by an interaction with other galaxies, it can form as a slow rotator, perhaps extending only to its inner Lindblad resonance (Lynden-Bell 1979; Combes & Elmegreen 1993; Miwa & Noguchi 1998).

Much weight has been given to the model-independent Tremaine-Weinberg (T-W) method (Tremaine & Weinberg 1984). It has been used to determine the pattern speeds of about 15 large-scale stellar bars. The results, which range from the unphysical $\mathcal{R} = 0.8$ to the slow-bar regime, with $\mathcal{R} = 1.8$, seem to be in accordance with fast bars, at least when the error estimates (typically larger for higher values of $\mathcal{R}$) are taken into account (Kent 1987; Merrifield & Kuijken 1995; Gerssen et al. 1999, 2003; Aguerri et al. 2003; Debattista & Williams 2004). This apparent lack of slow-rotating bars has been interpreted as indicating that the dark halos are dynamically insignificant in the inner parts of barred galaxies (Debattista & Sellwood 2000; Aguerri et al. 2003). This is in disagreement with some cosmological simulations of structure formation, which typically produce a centrally peaked dark matter component (Navarro et al. 1996). However, the application of the T-W method requires that one be able to measure a rigidly rotating component that satisfies the continuity equation. Thus, most measurements using stellar absorption-line spectrometry have been made for SB0 galaxies, which are almost free of gas and dust.

Although some attempts (Zimmer et al. 2004; Rand & Wallin 2004) have been made to use the T-W method with CO observations, the pattern speeds of late-type barred galaxies have usually been determined by various indirect methods. Models of individual galaxies with large-scale bars have usually produced small $\mathcal{R}$-estimates (Hunter et al. 1988; England 1989; England et al. 1990; Kaufmann & Contopoulos 1996; Lindblad et al. 1996), although some models that set $R_{\rm CR}$ well outside the bar radius have also been published (Sempere et al. 1995; Lindblad & Kristen 1996; Rautiainen et al. 2004). The situation is different for galaxies, where the bar is so small or weak that the spiral component probably dominates. In several cases, a low pattern speed has been determined by modeling or by connecting morphological features to resonances (Patsis et al. 1991; Elmegreen & Elmegreen 1995; Patsis et al. 1997b; Sempere & Rozas 1997; Aguerri et al. 1998; Kranz et al. 2003). If the bar and spiral have the same pattern speed in these systems, usually of late Hubble type, then their bars are slow rotators.

A major problem in interpreting the pattern-speed estimates is that the individual measurements have been carried out by different groups using different methods and are based on data of very uneven quality. In this Letter, we try to improve the situation by presenting a simulation series of 38 moderately inclined barred galaxies, using data from the Ohio State University Bright Galaxy Survey (OSUBGS; Eskridge et al. 2002). Our study represents the largest set of barred galaxies whose pattern speeds have been determined with a consistent method. Furthermore, the morphological types of these galaxies range from SB0/a to SBc, based on the Third Reference Catalogue of Bright Galaxies (RC3; de Vaucouleurs et al. 1991), so that several galaxies of each morphological type are included. Whereas we find all the bars of early-type galaxies (SBab or earlier) in the sample to be fast rotators, our models suggest that galaxies of later morphological types include both fast- and slow-rotating bars.

2. SIMULATIONS

Our modeling method is essentially the same as we used in modeling IC 4214 and ESO 566-24 (Salo et al. 1999; Rautiainen et al. 2004), with the exception that we do not have kinematic data for this larger sample. We assume that the H-band light distribution corresponds to the projected distribution of lumi-

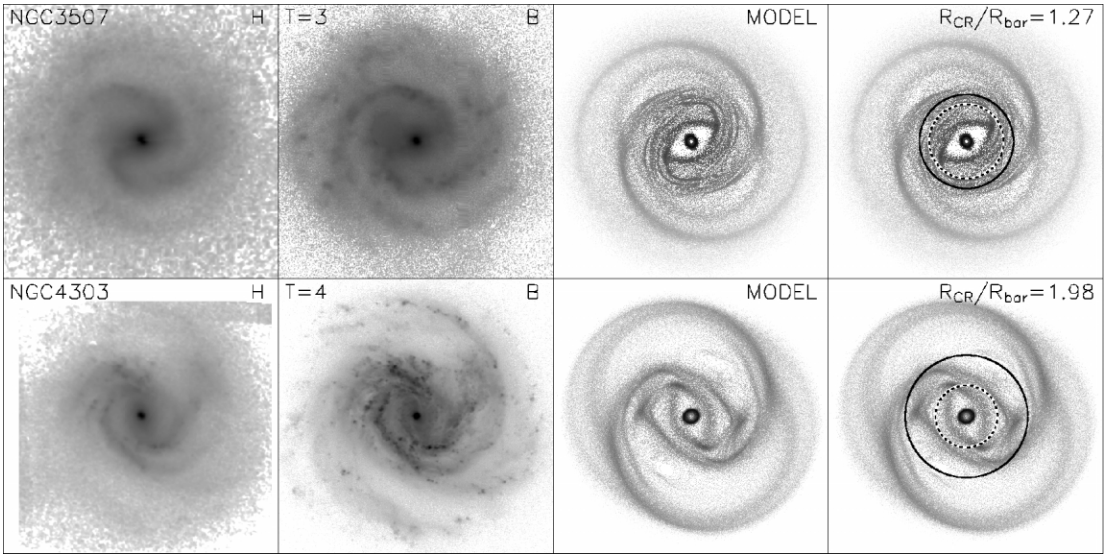

FIG. 1.—Two examples of our galaxy modeling: NGC 3507 and NGC 4303. The first panel in the top row shows the deprojected *H*-band image of NGC 3507, the second panel the *B*-band image, and the third the gas morphology in our best-fitting model. The final panel shows the gas morphology with overplotted $R_{\rm bar}$ and $R_{\rm CR}$ circles (*dashed and solid lines, respectively*). The bottom row shows similar images for NGC 4303.

nous matter (constant M/L) and that there is only one pattern speed in each galaxy.

The gravitational potentials that we use were calculated in Laurikainen et al. (2004), based on the *H*-band images from the OSUBGS. Thus, for each image the bulge component was first removed using a two-dimensional bulge-disk-bar decomposition, after which the disk was deprojected to a face-on orientation. The light distribution of the disk was approximated by a Fourier decomposition, and the disk gravity was calculated using the even azimuthal components from $m = 0$ to $m = 8$. An exponential vertical distribution was assumed, with a constant scale height throughout the disk; the scale height was chosen according to the morphological type of the galaxy, using the typical ratios of vertical to radial scale length given by de Grijs (1998). The gravitational potential of the bulge was added to the disk potential, assuming that the bulge mass is spherically distributed. For more details of the potential calculation, see Laurikainen & Salo (2002).

We simulated the behavior of two-dimensional disks of collisionless stellar test particles and inelastically colliding gas particles in the determined potentials. The main modeling parameter was the pattern speed of the nonaxisymmetric part of the potential. For more details on the simulation code, see Salo et al. (1999). As an alternative mass model, we also made simulations in which a dark halo component based on the universal rotation curve of Persic et al. (1996) was included in a similar manner as in Buta et al. (2004). To calculate the halo profile, we used $L/L_\star$ calculated with data from the RC3 and NED (the NASA/IPAC Extragalactic Database). The best-fitting pattern speed and a crude estimate of the error (typically we could determine $R_{\rm CR}$ with an accuracy of about $\pm 10\%$) was determined by visual comparison between the simulation morphology and the *B*- and *H*-band images. The lengths of the bars were determined by inspection of the deprojected *H*-band images, their isophotes, and the $m = 2$ Fourier phase angles. We estimate that the error in bar length is $\pm 10\%$, so that the typical error in $\mathcal{R}$ is about $\pm 20\%$.

The morphological features we used in the comparison are the spiral arms, the inner rings that surround the bar, and the outer rings. In a few cases we could not find a single best-fitting pattern speed because the outer parts favored a lower pattern speed than the inner parts did. A possible reason for this is that a galaxy might have more than one pattern speed, which is often seen in *N*-body simulations of barred galaxies (Sellwood & Sparke 1988; Masset & Tagger 1997; Rautiainen & Salo 1999). In such cases the value adopted corresponds to the smallest $\mathcal{R}$ (fastest bar), best characterizing the bar region.

Two examples of our modeling are shown in Figure 1. The main features of NGC 3507 are the bar and two very long spiral arms, which can be followed for almost 360°. Our best-fitting model, with $\mathcal{R} \approx 1.3$, reproduces the spiral structure over its full length. With a higher pattern speed, the simulated spiral winds too tightly and does not have the observed extent, whereas with a lower pattern speed the innermost spiral is not reproduced. The best-fitting model sets $R_{\rm bar}$ between the inner 4:1 resonance and corotation (the resonance radii are calculated from the azimuthally averaged potential). The end of the spiral is close to the outer Lindblad resonance (OLR). The second example, NGC 4303, has a spiral structure whose inner part consists of straight arm segments. This morphology is nicely reproduced when $\mathcal{R} \approx 2.0$, that is, the bar is slow. The strai ght segments disappear beyond the listed range of $\mathcal{R}$. The bar ends almost exactly in the inner 4:1 resonance, and the spiral extends to the OLR. The bright inner part of the spiral structure ends in the corotation. The innermost angle between straight arm segments is close to the inner 4:1 resonance, but the outer ones are close to 6:1 and 8:1 resonances. We will present detailed descriptions of our models and compare our results with several suggested morphological resonance indicators (e.g., Elmegreen & Elmegreen 1990; Elmegreen et al. 1992) in a forthcoming paper.

3. RESULTS AND DISCUSSION

Our modeling results are summarized in Table 1 and in Figure 2. There is a clear trend between the pattern speed and the Hubble stage T: the average value of $\mathcal{R}$ is about 1.1 for type SB0/a ($T = 0$), about 1.4 for SBb ($T = 3$), and 1.7 for SBc

TABLE 1
MODELING RESULTS FOR EACH GALAXY

Galaxy	R_{bar} (arcsec)	R_{CR} (arcsec)	ΔR_{CR} (arcsec)	R_{CR}/R_{bar} ($=\mathcal{R}$)	T
NGC 289	23.2	61.0	7.6	2.63	4
NGC 578	24.4	78.9	15.8	3.24	5
NGC 613	80.0	131.0	9.7	1.64	4
NGC 1073	51.0	48.7	4.4	0.95	5
NGC 1187	42.9	64.4	9.7	1.50	5
NGC 1241	31.5	41.5	4.0	1.32	3
NGC 1302	34.8	55.0	4.6	1.58	0
NGC 1317	53.4	51.9	7.8	0.97	1
NGC 1832	18.9	31.2	3.1	1.65	4
NGC 3261	30.0	46.3	2.2	1.54	3
NGC 3275	33.3	44.2	2.3	1.33	2
NGC 3504	39.0	44.5	5.6	1.14	2
NGC 3507	27.0	34.2	2.6	1.27	3
NGC 3513	30.0	38.1	2.7	1.27	5
NGC 3583	24.0	32.1	1.8	1.34	3
NGC 3686	25.5	33.0	5.1	1.30	4
NGC 3726	42.0	88.2	9.3	2.10	5
NGC 4051	58.5	98.0	7.0	1.68	4
NGC 4123	58.5	65.9	6.3	1.13	5
NGC 4303	45.0	89.1	8.5	1.98	4
NGC 4314	76.5	81.7	10.2	1.07	1
NGC 4394	46.5	66.7	10.0	1.43	3
NGC 4450	49.5	56.6	4.4	1.14	2
NGC 4457	45.0	39.9	2.8	0.89	0
NGC 4548	72.0	95.2	11.9	1.32	3
NGC 4579	46.5	71.1	8.4	1.53	3
NGC 4643	67.5	69.1	4.6	1.02	0
NGC 4665	60.0	55.2	7.9	0.92	0
NGC 4902	26.6	44.3	4.4	1.66	3
NGC 4930	46.6	46.6	3.9	1.00	3
NGC 4995	28.5	64.2	5.5	2.25	3
NGC 5701	50.0	59.2	5.4	1.19	0
NGC 5850	75.0	105.1	5.8	1.40	3
NGC 5921	51.0	78.5	7.1	1.54	4
NGC 6384	30.0	72.5	8.1	2.42	4
NGC 6782	31.3	37.1	2.6	1.18	1
NGC 7552	67.3	65.0	5.9	0.97	2
NGC 7723	25.5	33.5	4.2	1.31	3

($T = 5$). Thus, the bars of the early-type galaxies are typically fast rotators, whereas those of the late types are slow rotators. This trend is not conclusive: all morphological types include galaxies with $\mathcal{R} \approx 1$.

This trend between Hubble stage and pattern speed might be related to the bar size. Based on the error estimates for R_{CR} and R_{bar}, we can deem six galaxies out of 18 with $\mathcal{R} > 1.4$ as "definitely slow-rotating," that is, $\mathcal{R} - \Delta\mathcal{R} > 1.4$. If we follow Elmegreen & Elmegreen's (1995) division into large and small bars, then five of these galaxies have a small bar ($R_{bar}/R_{25} < 0.3$). Indeed, the three galaxies with the highest value of $\mathcal{R}$, NGC 289, NGC 578, and NGC 6384, are also the three with the smallest bars when compared with the galaxy size ($R_{bar}/R_{25} = 0.15$–0.17). In NGC 289 and NGC 578, the innermost structure would also allow a higher pattern speed, but even then $\mathcal{R}$ would be much larger than 1.4. In NGC 6384, the very long spiral structure is completely reproduced with the listed value of $\mathcal{R}$, whereas a fast-rotating bar can reproduce only the innermost part of the spiral. NGC 3726 and NGC 4303 (see pre vious section) have $R_{bar}/R_{25} \approx 0.23$, which does not differ considerably from several other galaxies with a lower value of $\mathcal{R}$. The inner structure of NGC 3726 also allows a fast-bar solution, but the overall morphology, including the inner ring, is better reproduced with the value listed in Table 1. In the case of NGC 4995, the fit is not very good, and a value giving a fast-rotating bar cannot be excluded. Whereas the range $0.2 < R_{bar}/R_{25} < 0.4$ includes both fast- and slow-rotating bars, the galaxies with $R_{bar}/R_{25} > 0.4$ are fast rotators with only one exception, NGC 613, for which the fit was also poor.

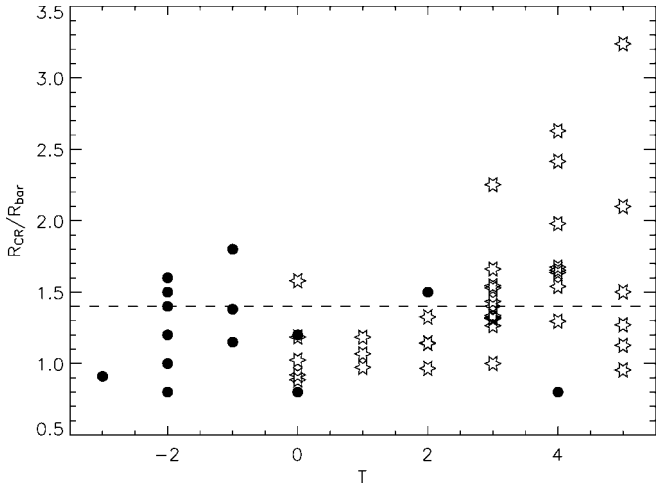

FIG. 2.—Ratio R_{CR}/R_{bar} as a function of Hubble stage T. The stars show our modeling results, and the circles show the pattern-speed estimates with the T-W method applied to stellar absorption lines. The dashed line shows the dividing line between fast and slow bars, $R_{CR}/R_{bar} = 1.4$.

We found previously published pattern-speed estimates for eight galaxies in our sample. Unfortunately, none of these was based on the direct T-W method; instead, either morphological arguments or simulation modeling was used to determine $\mathcal{R}$ (for NGC 1073 and NGC 4123 we found both morphological and model-based estimates of the pattern speed). In three cases, NGC 1073, NGC 4123, and NGC 5921, R_{CR} was estimated by the method of Puerari & Dottori (1997) (Aguerri et al. 1998): the B- and I-band $m = 2$ phase-angle crossing is identified to be a signature of the CR, giving $\mathcal{R}$-values of 1.17, 1.41, and 1.28, respectively. For NGC 613 (Elmegreen et al. 1992) and NGC 3504 (Kenney et al. 1993), the morphological signatures of the OLR (extent of the spiral structure, the outer ring) and the rotation curves were used to determine R_{CR} (in both cases corresponding to $\mathcal{R} = 1.0$). Aguerri et al. (2000) determined $\mathcal{R} = 1.0$ for NGC 7723 by assuming that the corotation region lacked recent star formation. Three galaxies, NGC 1073, NGC 4123, and NGC 5850, have previously been modeled by England et al. (1990), Weiner et al. (2001), and Aguerri et al. (2001), respectively, and for NGC 4314 the pattern speed was found by matching the shapes of particle orbits with the observed outer ring (Quillen et al. 1994; Patsis et al. 1997a). Altogether, in five cases out of eight a smaller value of $\mathcal{R}$ was found than in our study, and in three cases a larger one. For only two galaxies was the difference larger than our typical error estimate, $\pm 20\%$. If we take into account differences in the adopted bar lengths and orientation parameters, our pattern-speed determinations are in good accordance with the previous estimates for these galaxies. However, only now, using a large sample of galaxies, a clear systematic trend can be found.

Strictly speaking, our results are not in disagreement with those obtained with the T-W method. Namely, the measurements with the T-W method have been limited to early-type barred galaxies, which indeed have fast bars. They have sometimes been considered to represent the whole population of barred galaxies, which does not seem to be justified. In particular, the slow bars in our sample could be systems in

which the angular momentum transfer between the bar and a dark halo with substantial central density has slowed down the bar's rotation. Alternatively, the difference in pattern speeds could be primordial: early-type galaxies with massive bulges may favor the formation of fast bars.

In the future, it will be important to extend the overlap of pattern-speed estimates based on different methods, both by applying the current modeling to earlier-type galaxies (e.g., using data from the ongoing survey of S0 galaxies; Laurikainen et al. 2005) and by extending the direct measurements to later types. This would give a better picture of the accuracy and possible biases of the pattern-speed determinations.

We thank the referee for very useful suggestions. This research has made use of the NASA/IPAC Extragalactic Database, which is operated by the Jet Propulsion Laboratory, California Institute of Technology, under contract with the National Aeronautics and Space Administration.

REFERENCES

Aguerri, J. A. L., Beckman, J. E., & Prieto, M. 1998, AJ, 116, 2136
Aguerri, J. A. L., Debattista, V. P., & Corsini, E. Mª. 2003, MNRAS, 338, 465
Aguerri, J. A. L., Hunter, J. H., Prieto, M., Varela, A. M., Gottesman, S. T., & Muñoz-Tuñón, C. 2001, A&A, 373, 786
Aguerri, J. A. L., Muñoz-Tuñón, C., Varela, A. M., & Prieto, M. 2000, A&A, 361, 841
Athanassoula, E. 2003, MNRAS, 341, 1179
Buta, R., Laurikainen, E., & Salo, H. 2004, AJ, 127, 279
Combes, F., & Elmegreen, B. G. 1993, A&A, 271, 391
Contopoulos, G. 1980, A&A, 81, 198
de Grijs, R. 1998, MNRAS, 299, 595
de Vaucouleurs, G., de Vaucouleurs, A., Corwin, H. G., Jr., Buta, R. J., Paturel, G., & Fouqué, P. 1991, Third Reference Catalogue of Bright Galaxies (Berlin: Springer)
Debattista, V. P., & Sellwood, J. A. 1998, ApJ, 493, L5
———. 2000, ApJ, 543, 704
Debattista, V. P., & Williams, T. B. 2004, ApJ, 605, 714
Elmegreen, B. G., & Elmegreen, D. M. 1990, ApJ, 355, 52
Elmegreen, B. G., Elmegreen, D. M., & Montenegro, L. 1992, ApJS, 79, 37
Elmegreen, D. M., & Elmegreen, B. G. 1995, ApJ, 445, 591
England, M. N. 1989, ApJ, 344, 669
England, M. N., Gottesman, S. T., & Hunter, J. H., Jr. 1990, ApJ, 348, 456
Eskridge, P. B., et al. 2002, ApJS, 143, 73
Gerssen, J., Kuijken, K., & Merrifield, M. R. 1999, MNRAS, 306, 926
———. 2003, MNRAS, 345, 261
Hunter, J. H., Jr., Ball, R., Huntley, J. M., England, M. N., & Gottesman, S. T. 1988, ApJ, 324, 721
Kaufmann, D. E., & Contopoulos, G. 1996, A&A, 309, 381
Kenney, J. D. P., Carlstrom, J. E., & Young, J. S. 1993, ApJ, 418, 687
Kent, S. M. 1987, AJ, 93, 1062
Kranz, T., Slyz, A., & Rix, H.-W. 2003, ApJ, 586, 143
Laurikainen, E., & Salo, H. 2002, MNRAS, 337, 1118
Laurikainen, E., Salo, H., & Buta, R. 2005, MNRAS, 362, 1319
Laurikainen, E., Salo, H., Buta, R., & Vasylyev, S. 2004, MNRAS, 355, 1251
Lindblad, P. A. B., & Kristen, H. 1996, A&A, 313, 733
Lindblad, P. A. B., Lindblad, P. O., & Athanassoula, E. 1996, A&A, 313, 65
Lynden-Bell, D. 1979, MNRAS, 187, 101
Masset, F., & Tagger, M. 1997, A&A, 322, 442
Merrifield, M. R., & Kuijken, K. 1995, MNRAS, 274, 933
Miwa, T., & Noguchi, M. 1998, ApJ, 499, 149
Navarro, J. F., Frenk, C. S., & White, S. D. M. 1996, ApJ, 462, 563
Patsis, P. A., Athanassoula, E., & Quillen, A. C. 1997a, ApJ, 483, 731
Patsis, P. A., Contopoulos, G., & Grosbøl, P. 1991, A&A, 243, 373
Patsis, P. A., Grosbøl, P., & Hiotelis, N. 1997b, A&A, 323, 762
Persic, M., Salucci, P., & Stel, F. 1996, MNRAS, 281, 27 (erratum 283, 1102)
Puerari, I., & Dottori, H. 1997, ApJ, 476, L73
Quillen, A. C., Frogel, J. A., & González, R. A. 1994, ApJ, 437, 162
Rand, R. J., & Wallin, J. F. 2004, ApJ, 614, 142
Rautiainen, P., & Salo, H. 1999, A&A, 348, 737
Rautiainen, P., Salo, H., & Buta, R. 2004, MNRAS, 349, 933
Salo, H., Rautiainen, P., Buta, R., Purcell, G. B., Cobb, M. L., Crocker, D. A., & Laurikainen, E. 1999, AJ, 117, 792
Sellwood, J. A. 1981, A&A, 99, 362
Sellwood, J. A., & Sparke, L. S. 1988, MNRAS, 231, 25P
Sempere, M. J., García-Burillo, S., Combes, F., & Knapen, J. H. 1995, A&A, 296, 45
Sempere, M. J., & Rozas, M. 1997, A&A, 317, 405
Tremaine, S., & Weinberg, M. D. 1984, ApJ, 282, L5
Weiner, B. J., Sellwood, J. A., & Williams, T. B. 2001, ApJ, 546, 931
Zimmer, P., Rand, R. J., & McGraw, J. T. 2004, ApJ, 607, 285